26

Modeling Spatial Trajectories

David R. Brillinger

CONTENTS

26.1 Introduction

The study of trajectories has been basic to science for many centuries. One can mention the motion of the planets, the meanderings of animals and the routes of ships. More recently there has been considerable modeling and statistical analysis of biological and ecological processes of moving particles. The models may be motivated formally by difference and differential equations and by potential functions. Initially, following Liebnitz and Newton, such models were described by deterministic differential equations, but variability around observed paths has led to the introduction of random variables and to the development of stochastic calculi. The results obtained from the fitting of such models are highly useful. They may be employed for: simple description, summary, comparison, simulation, prediction, model appraisal, bootstrapping, and also employed for the estimation of derived quantities of interest. The potential function approach, to be presented in section 26.3.4, will be found to have the advantage that an equation of motion is set down quite directly and that explanatories, including attractors, repellors, and time-varying fields may be included conveniently.

Movement process data are being considered in novel situations: assessing Web sites, computer-assisted surveys, soccer player movements, iceberg motion, image scanning, bird navigation, health hazard exposure, ocean drifters, wildlife movement. References showing the variety and including data analyses include: [4,9,14,17,19,21,27,29,33–35,39,40]. In the chapter, consideration is given to location data $\{\mathbf{r}(t_i),\ i = 1, \dots, n\}$ and models leading to such data. As the notation implies and practice shows, observation times, $\{t_i\}$, may be un-equally spaced. The chapter also contains discussion of inclusion of explanatory variables. It starts with the presentation and discussion of two empirical examples of trajectory data. The first refers to the motion of a small particle moving about in a fluid and the second to the satellite-determined locations of a Hawaiian monk seal foraging off the island of Molokai. The following material concerns pertinent stochastic models for trajectories and some of their properties. It will be seen that stochastic differential equations (SDEs) are useful for motivating models and that corresponding inference procedures have been developed. In particular, discrete approximations to SDEs lead to likelihood functions and, hence, classic confidence and testing procedures become available.

The basic motivation for the chapter is to present a unified approach to the modeling and analysis of trajectory data.

26.2 History and Examples

26.2.1 Planetary Motion

Newton derived formal laws for the motion of the planets and further showed that Kepler's Laws could be derived from these. Lagrange set down a potential function and Newton's equations of motion could be derived from it in turn. The work of Kepler, Newton and Lagrange has motivated many models in physics and engineering. For example, in a study describing the motion of a star in a stellar system, Chandrasekhar [11] sets down equations of the form

$$\frac{d\mathbf{u}(t)}{dt} = -\beta\mathbf{u}(t) + \mathbf{A}(t) + \mathbf{K}(\mathbf{r}(t), t) \tag{26.1}$$

with $\mathbf{u}$, velocity; $\mathbf{A}$, a Brownian-like process; β, a coefficient of friction; and $\mathbf{K}$, the acceleration produced by an external force field. Chandresekar in [11] refers to this equation as a generalized Langevin equation. It is an example of an SDE.

Next, two examples of empirical trajectory data are presented.

26.2.2 Brownian Motion

In general science, Brownian motion refers to the movement of tiny particles suspended in a liquid. The phenomenon is named after Robert Brown, an Englishman, who in 1827 carried out detailed observations of the motion of pollen grains suspended in water [17]. The phenomenon was modeled by Einstein. He considered the possibility that formalizing Brownian motion could support the idea that molecules existed. Langevin [26] set down the following expression for the motion of such a particle,

$$m\frac{d^2x}{dt^2} = -6\pi\mu a\frac{dx}{dt} + X,$$
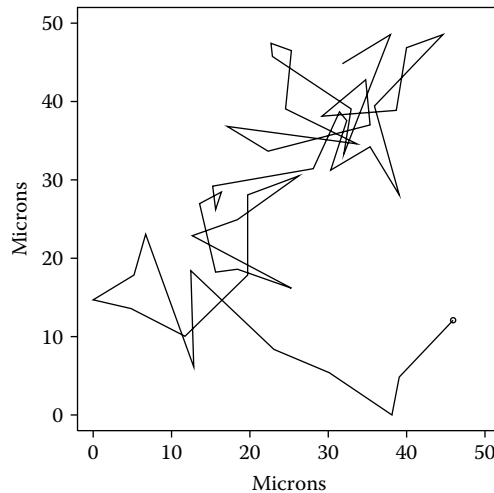
FIGURE 26.1
Perrin's measurements of the location of a mastic grain at 48 successive times. The figure is adapted from one in [16].

where m is the particle's mass, a is its radius of the particle, μ is the viscosity of the liquid, and X is the "complementary force"—a Brownian process-like term. One can view this as an example of an SDE.

A number of "Brownian" trajectories were collected by Perrin [31]. One is provided in Figure 26.1 and the results of an analysis will be presented later in the chapter. The particles involved were tiny mastic grains with a radius of .53 microns. Supposing (x, y) refers to position in the plane, the trajectory may be written $(x(t), y(t)), t = 1, \ldots, 48$. The time interval between the measurements in this case was 30 sec.

In Figure 26.1, one sees the particle start in the lower right corner of the figure and then meander around a diagonal line running from the lower left to the upper right.

26.2.3 Monk Seal Movements

The Hawaiian monk seal is an endangered species. It numbers only about 1,400 today. They are now closely monitored, have a life span of about 30 years, weigh between 230 and 270 kilos and have lengths of 2.2 to 2.5 meters.

Figure 26.2 shows part of the path of a juvenile female monk seal swimming off the southwest coast of the island of Molokai, Hawaii. Locations of the seal as it moved and foraged were estimated from satellite detections, the animal having a radio tag glued to its dorsal fin. The tag's transmissions could be received by satellites passing overhead when the animal was on the surface. The animal's position could then be estimated.

The data cover a period of about 15 days. The seal starts on a beach on the southwest tip of Molokai and then heads to the far boundary of a reserve called Penguin Bank, forages there for a while, and then heads back to Molokai, perhaps to rest in safety. Penguin Bank is indicated by the dashed line in the figure.

An important goal of the data collection in this case was the documentation of the animals' geographic and vertical movements as proxies of foraging behavior and then to use this information to assist in the survival of the species. More detail may be found in [9] and [40].
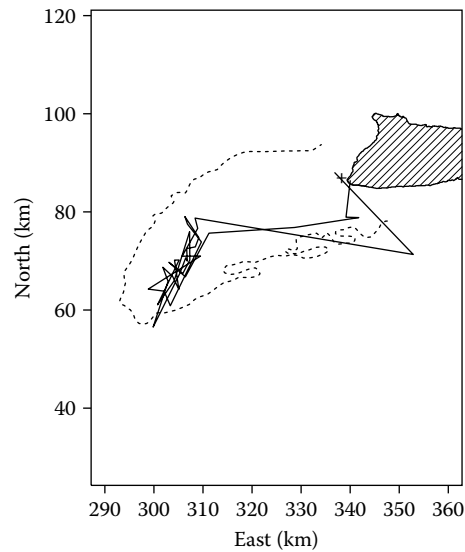
FIGURE 26.2
Estimated locations of a Hawaiian monk seal off the coast of Molokai. The dashed line is the 200 fathom line, approximately constraining an area called the Penguin Bank Reserve.

26.3 Statistical Concepts and Models

26.3.1 Displays

It is hard to improve on visual displays in studies of trajectory data. In a simple case, one shows the positions $(x(t_i), y(t_i))$, $i = 1, 2, \ldots$, as a sequence of connected straight lines, as in Figure 26.1 and Figure 26.2. One can superpose other spatial information as a background. An example is Figure 26.2, which shows the outlines of Molokai, the hatched region, and Penguin Bank, the dashed line.

A related type of display results if one estimates a bivariate density function from the observed locations $(x(t_i), y(t_i))$, $i = 1, 2, \ldots$, and shows the estimate in contour or image form. Such figures are used in home range estimation; however, this display loses the information on where the animal was at different times.

A bagplot [36] is useful in processing trajectory data if estimated locations can be in serious error. It highlights the "middle 50%" of a bivariate dataset and is an extension of the univariate boxplot. An example is provided in [9]. Before preparing the bagplot presented there, this author did not know of the existence of the Penguin Bank Reserve. Computing the bagplot of all the available locations found the reserve.

Another useful display is a plot of the estimated speed of the particle versus time. One graphs the approximate speeds,

$$\sqrt{(x(t_{i+1}) - x(t_i))^2 + (y(t_{i+1}) - y(t_i))^2}/(t_{i+1} - t_i)$$

versus the average of the times, t_i and t_{i+1}, say. It is to be remembered that this "speed" provides only the apparent speed, not the instantaneous. The particle may follow a long route getting from $\mathbf{r}(t_i)$ to $\mathbf{r}(t_{i+1})$.

Figures are presented in this chapter, but videos can assist the analyses.

26.3.2 Autoregressive Models

A bivariate time series model that is coordinate free provides a representation for processes whose realizations are spatial trajectories. One case is the simple random walk,

$$\mathbf{r}_{t+1} = \mathbf{r}_t + \epsilon_{t+1}, \quad t = 0, 1, 2, \ldots$$

with $\mathbf{r}_0$ the starting point and $\{\epsilon_t\}$ a bivariate time series of independent and identically distributed variates.

In the same vein one can consider the bivariate order 1, autoregressive, VAR(1), given by

$$\mathbf{r}_{t+1} = \mathbf{a}\mathbf{r}_t + \epsilon_{t+1}, \quad t = 0, 1, 2, \ldots \tag{26.2}$$

for an **a** leading to stationarity.

The second difference of the motion of an iceberg has been modeled as an autoregressive in [29].

26.3.3 Stochastic Differential Equations

The notion of a continuous time random walk may be formalized as a formal Brownian motion. This is a continuous time process with the property that disjoint increments, $d\mathbf{B}(t)$, are independent Gaussians with covariance matrix $\mathbf{I}dt$. Here $\mathbf{B}(t)$ takes values in R^2. The random walk character becomes clear if one writes

$$\mathbf{B}(t + dt) = \mathbf{B}(t) + d\mathbf{B}(t), \quad -\infty < t < \infty.$$

The vector autoregressive of order 1 series may be seen as an approximation to a stochastic differential equation by writing

$$\mathbf{r}(t + dt) - \mathbf{r}(t) = \mu\mathbf{r}(t)dt + \sigma d\mathbf{B}(t)$$

and comparing it to Equation (26.2).

Given a Brownian process **B**, consider a trajectory **r** in R^2 that at time t has reached the position $\mathbf{r}(t)$ having started at $\mathbf{r}(0)$. Consider the "integral equation"

$$\mathbf{r}(t) = \mathbf{r}(0) + \int_0^t \mu(\mathbf{r}(s), s)ds + \int_0^t \sigma(\mathbf{r}(s), s)d\mathbf{B}(s) \tag{26.3}$$

with $\mathbf{r}, \mu, d\mathbf{B}$ each 2-vectors and σ 2 by 2. Here, μ is called the drift and σ the diffusion coefficient. Equation (26.3) is known as Ito's integral equation.

This equation requires the formal definition of the Ito integral

$$\int_a^b \mathbf{G}(\mathbf{r}(t), t)d\mathbf{B}(t)$$

for conformal **G** and **B**. Under regularity conditions, the Ito integral can be defined as the limit in mean-squared, as $\triangle \downarrow 0$, of

$$\sum_{j=1}^{N-1} \mathbf{G}(\mathbf{r}(t_j), t_j)[\mathbf{B}(t_{j+1}) - \mathbf{B}(t_j)],$$

where

$$a = t_1^{\triangle} < t_2^{\triangle} < \cdots < t_N^{\triangle} = b, \quad \triangle = max(t_{j+1} - t_j).$$

Expressing Equation (26.3) as an "Ito integral" is a symbolic gesture, but the definition is mathematically consistent.

The equation (26.3) is often written

$$d\mathbf{r}(t) = \mu(\mathbf{r}(t), t)dt + \sigma(\mathbf{r}(t), t)d\mathbf{B}(t) \tag{26.4}$$

using differentials, but Equation (26.3) is the required formal expression. For details on Ito integrals, see [12] or [15].

26.3.4 Potential Function Approach

A potential function is an entity from Newtonian mechanics. It leads directly to equations of motion in the deterministic case (see [41]). An important property is that a potential function is real-valued and thereby leads to a simpler representations for a drift function, μ, than those based on the vector-valued velocities.

To make this apparent, define a gradient system as a system of differential equations of the form

$$d\mathbf{r(t)}/dt = -\nabla V(\mathbf{r}(t)), \tag{26.5}$$

where $V : R^2 \rightarrow R$ is a differentiable function and $\nabla V = (\partial V/\partial x, \partial V/\partial y)^T$ denotes its gradient. ("T" here denotes transpose.) The negative sign in this system is traditional. The structure $d\mathbf{r}(t)/dt$ is called a vector field, while the function V is called a potential function.

The classic example of a potential function is the gravitational potential in R^3, $V(\mathbf{r}) = -G/ \mid \mathbf{r} - \mathbf{r}_0 \mid$ with G the constant of gravitation (see [11]). This function leads to the attraction of an object at position $\mathbf{r}$ toward the position $\mathbf{r}_0$. The potential value at $\mathbf{r} = \mathbf{r}_0$ is $-\infty$ and the pull of attraction is infinite there. Other specific formulas will be indicated shortly.

In this chapter the deterministic equation (26.5) will be replaced by a stochastic differential equation

$$d\mathbf{r}(t) = -\nabla V(\mathbf{r}(t))dt + \sigma(\mathbf{r}(t))d\mathbf{B}(t) \tag{26.6}$$

with $\mathbf{B}(t)$ a two-dimensional standard Brownian process, V a potential function, and σ a diffusion parameter. Under regularity conditions, a unique solution of such an equation exists and the solution process $\{\mathbf{r}(t)\}$ is Markov. Repeating a bit, a practical advantage of being able to write $\mu = -\nabla V$ is that V is real-valued and thereby simpler to model, to estimate, and to display.

For motion in R^2, the potential function is conveniently displayed in contour, image, or perspective form. Figure 26.3 and Figure 26.4 provide examples of image plots. If desired, the gradient may be displayed as a vector field. (Examples may be found in [6].)

An estimated potential function may be used for: simple description, summary, comparison, simulation, prediction, model appraisal, bootstrapping, and employed for the estimation of related quantities of interest. The potential function approach can handle attraction, and repulsion from points and regions directly. While the figures of estimated potential functions usually look like what you expect a density function to be, given the tracks, but there is much more to the potential surface; for example, the slopes are direction and speed of motion.

Some specific potential function forms that have proven useful are listed below. A research issue is how to choose among them and others. Subject matter knowledge can prove essential in doing this. To begin, consider the function

$$V(\mathbf{r}) = \alpha log\ d + \beta d \tag{26.7}$$

with $\mathbf{r} = (x, y)^T$ the location of a particle, and $d = d(\mathbf{r})$ the distance of the particle from a specific attractor. This function is motivated by equations in [21]. The attractor may move in

space in time, and then the potential function is time-dependent. Another useful functional form is

$$V(\mathbf{r}) = \gamma_1 x + \gamma_2 y + \gamma_{11} x^2 + \gamma_{12} xy + \gamma_{22} y^2 + C/d_M, \tag{26.8}$$

where $d_M = d_M(x, y)$ is the distance from location (x, y) to the nearest point of a region, M, of concern. Here, with $C > 0$, the final term keeps the trajectory out of the region. On the other hand,

$$V(\mathbf{r}) = \alpha \log d + \beta d + \gamma_1 x + \gamma_2 y + \gamma_{11} x^2 + \gamma_{12} xy + \gamma_{22} y^2, \tag{26.9}$$

where $d = d(\mathbf{r}) = d(x, y)$ is the shortest distance to a point, leads to attraction to the point as well as providing some general structure. It is useful to note for computations that the expressions (26.7) to (26.9) are linear in the parameters.

In summary, the potential function approach advocated here is distinguished from traditional SDE-based work by the fact that μ has the special form (26.5).

26.3.5 Markov Chain Approach

Taking note of the work of [22], [23], and [24], it is possible to approximate the motion implied by an SDE, of a particle moving in R^2, by a Markov chain in discrete time and space. This can be useful for both simulations of the basic process and for intuitive understanding.

In the approach of [23] and [24], one sets up a grid forming pixels, and then makes a Markov chain assumption. Specifically define

$$\mathbf{a}(\mathbf{r}, t) = \frac{1}{2}\sigma(\mathbf{r}, t)\sigma(\mathbf{r}, t)^T$$

and, for convenience of exposition here, suppose that $a_{ij}(\mathbf{r}, t) = 0$, $i \neq j$, i.e., the error components of the Gaussian vector are assumed statistically independent for fixed $\mathbf{r}$. Suppose further that time is discretized with $t_{k+1} - t_k = \Delta$. Write $\mathbf{r}_k = \mathbf{r}(t_k)$, and suppose that the lattice points of the grid have separation h. Let $\mathbf{e}_i$ denote the unit vector in i-th coordinate direction, $i = 1, 2$. Now consider the Markov chain with transition probabilities,

$$P(\mathbf{r}_k = \mathbf{r}_0 \pm \mathbf{e}_i h \mid \mathbf{r}_{k-1} = \mathbf{r}_0)$$
$$= \frac{\Delta}{h^2}(a_{ii}(\mathbf{r}_0, t_{k-1}) + h|\mu_i(\mathbf{r}_0, t_k - 1)|^{\pm})$$
$$P(\mathbf{r}_k = \mathbf{r}_0 \mid \mathbf{r}_{k-1} = \mathbf{r}_0) = 1 - \sum preceding.$$

Here it is supposed the probabilities are ≥ 0, which may be arranged by choice of Δ and h. In the above expressions the following notation has been employed:

$$|u|^+ = u \text{ if } u > 0 \text{ and } = 0 \text{ otherwise}$$

and

$$|u|^- = -u \text{ if } u < 0 \text{ and } = 0 \text{ otherwise}.$$

A discrete random walk is the simplest case of this construction.

(For results on the weak convergence of such approximations to SDEs, see [12], [22], and [23].)

With that introduction attention can turn to a different, yet related type of model. Suppose that a particle is moving along the points of a lattice in R^2 with the possibility of moving one step to the left or one to the right or one step up or one step down. View the lattice as the state space of a Markov chain in discrete time with all transition probabilities 0 except for the listed one step ones. This is the structure of the just provided approximation. The difference is that one will start by seeking a reasonable model for the transition probabilities directly, rather than coefficients for SDE.

26.4 Inference Methods

There is substantial literature devoted to the topic of inference for stochastic differential equations (references include [32], [37]). Many interesting scientific questions can be posed and addressed involving them and their applications. Elementary ones include: Is a motion Brownian? Is it Brownian with drift? These can be formulated in terms of the functions μ and σ of Equation (26.3) and Equation (26.4).

Consider an object at position $\mathbf{r}(t)$ in R^2 at time t. In terms of approximate velocity, Equation (26.6) leads to

$$(\mathbf{r}(t_{i+1}) - \mathbf{r}(t_i))/(t_{i+1} - t_i) = -\nabla V(\mathbf{r}(t_i)) + \sigma \mathbf{Z}_{i+1}/\sqrt{t_{i+1} - t_i} \qquad (26.10)$$

with the $\mathbf{Z}_i$ independent and identically distributed bivariate, standard normals. The reason for the $\sqrt{t_{i+1} - t_i}$ is that for real-valued Brownian $Var(dB(t)) = \sigma\, dt$. In Equation (26.10), one now has a parametric or nonparametric regression problem for learning about V, depending on the parametrization chosen. If the t_i are equispaced, this is a parametric or nonparametric autoregression model of order 1.

If desired, the estimation may be carried out by ordinary least squares or maximum likelihood depending on the model and the distribution chosen for the $\mathbf{Z}_i$. The naive approximation (26.10) is helpful for suggesting methods. It should be effective if the time points, t_i, are close enough together. In a sense (26.10), not (26.3), has become the model of record.

To be more specific, suppose that μ has the form

$$\mu(\mathbf{r}) = g(\mathbf{r})^T \beta$$

for an L by 1 parameter β and a p by L known function g. This assumption, from Equation (26.10) leads to the linear regression model

$$\mathbf{Y}_n = \mathbf{X}_n \beta + \epsilon_n$$

having stacked the $n-1$ values $(\mathbf{r}(t_{i+1}) - \mathbf{r}(t_i))/\sqrt{t_{i+1} - t_i}$ to form the $(n-1)p$ vector $\mathbf{Y}_n$, stacked the $n-1$ matrices $\mu(\mathbf{r}(t_i), t_i)\sqrt{(t_{i+1} - t_i)}$ to form the $(n-1)p$ by L matrix $\mathbf{X}_n$ and stacked the $n-1$ values $\sigma \mathbf{Z}_{i+1}$ to form ϵ_n. One is thereby led to consider the estimate

$$\hat{\beta} = \left(\mathbf{X}_n^T \mathbf{X}_n\right)^{-1} \mathbf{X}_n^T \mathbf{Y}_n$$

assuming the indicated inverse exists. Continuing, one is led to estimate $g(\mathbf{r})^T \beta$ by $g(\mathbf{r})^T \hat{\beta}$.

Letting y_j denote the jth entry of $\mathbf{Y}_n$ and $\mathbf{x}_j^T$ denote the jth row of $\mathbf{X}_n$, one can compute

$$s_n^2 = ((n-1)p^{-1} \sum \left(y_j - \mathbf{x}_j^T \hat{\beta}\right)^T \left(y_j - \mathbf{x}_j^T \hat{\beta}\right),$$

as estimate of σ^2 and, if desired, proceed to form approximate confidence intervals for the value $g(\mathbf{r})^T \beta$ using the results of [25]. In particular, the distribution of

$$\left(g(\mathbf{r})^T \left(\mathbf{X}_n^T \mathbf{X}_n\right)^{-1} g(\mathbf{r})\right)^{-1/2} g(\mathbf{r})^T (\hat{\beta} - \beta)/s_n$$

may be approximated by a standard normal for large n. (Further details may be found in [5].)

Another concern is deciding on the functional form for the drift terms μ and the diffusion coefficient σ of the motivating model (26.3). In [35], [6] the estimates are nonparametric.

26.5 Difficulties That Can Arise

One serious problem that can arise in work with trajectory data relates to the uncertainty of the location estimates. The commonly used Loran and satellite-based estimated locations can be in serious error. The measurement errors have the appearance of including outliers rather than coming from some smooth long-tailed distribution. In the monk seal example, the bagplot proved an effective manner to separate out outlying points. It led to the empirical discovery of the Penguin Bank Reserve in the work. Improved estimates of tracks may be obtained by employing a state space model and robust methods (see [1] and [20]).

A difficulty created by introducing the model via an SDE is that some successive pairs of time points, $t_i - t_{i-1}$, may be far apart. The concern arises because the model employed in the fitting is (26.10). One can handle this by viewing Equation (26.10) as the model of record, forgetting where it came from, and assessing assumptions, such as the normality of the errors, by traditional methods.

It has already been noted above that the speed estimate is better called the apparent speed estimate because one does not have information on the particle's movement between times t_{i-1} and t_i. Correction terms have been developed for some cases [18].

26.6 Results for the Empirical Examples

Figure 26.3 provides the estimated potential function, $\hat{V}$, for Perrin's data assuming the functional form (26.8) with $C = 0$. The particle's trajectory has been superposed in the figure. One sees the particle being pulled toward central elliptical regions and remaining
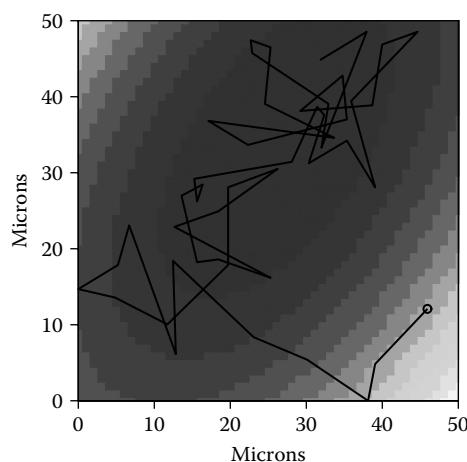

FIGURE 26.3
The estimated potential function for the Perrin data using the form (26.8) with $C = 0$. The circle represents the initial location estimate.
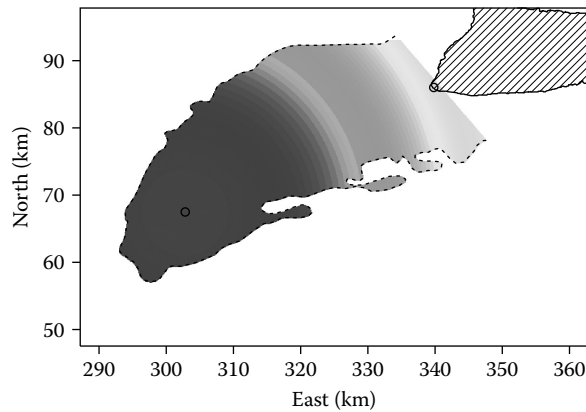
FIGURE 26.4
A potential function estimate computed to describe a Hawaiian monk seal's outbound, then inbound, foraging journeys from the southwest corner of Molokai. The circle in the southwest corner represents an assumed point of attraction.

in or nearby. This nonrandom behavior could have been anticipated from the presence of viscosity in the real world [17]. Were the process "pure" Brownian, the particle would have meandered about totally randomly and the SDE been

$$d\mathbf{r}(t) = \sigma d\mathbf{B}(t).$$

The Smolukowski approximation (see [11],[30]), takes (26.1) into

$$d\mathbf{r}(t) = \mathbf{K}(\mathbf{r}(t), t)dt/\beta + \sigma \mathbf{B}(t)$$

instead. The backgound in Figure 26.3 is evidence against the pure Brownian model for Perrin's data.

Figure 26.4 concerns the outbound foraging journeys of a Hawaiian monk seal whose outbound and inbound parts of one journey were graphed in Figure 26.2. Figure 26.4 is based on a trajectory including five journeys. The animal goes out apparently to forage and then returns to rest and be safer. The potential function employed is Equation (26.9) containing a term, $\alpha log(d) + \beta d$, that models attraction of the animal out to the far part of Penguin Bank Reserve. More detail on this analysis may be found in [9]. Outbound journeys may be simulated using the fitted model and hypotheses may be addressed formally.

26.7 Other Models

Figure 26.4 shows the western coast of the island of Molokai. Coasts provide natural boundaries to the movements of the seals. In an analysis of the trajectory of a different animal, that seal is kept off Molokai in the modeling by taking $C > 0$ in the final term in (26.8, see [8]).

Please clarify for sense.

A boundary is an example of an explanatory variable and it may be noted that there is now substantial literature on SDEs with boundaries [3]. There are explanatory variables to be included. A particle may be moving in a changing field $G(\mathbf{r}(t), t)$ and one is led to write

$$d\mathbf{r} = \mu dt + \gamma \nabla G + \sigma d\mathbf{B}.$$

A case is provided by sea surface height (SSH) with the surface currents given by the gradient of the SSH field. It could be that $\mu = -\nabla V$ as previously noted in this chapter.

A different type of explanatory, model and analysis is provided in [7]. The moving object is an elk and the explanatory is the changing location, $\mathbf{x}(t)$ of an all terrain vehicle (ATV). The noise of an ATV is surely a repellor when it is close to an elk, but one wonders at what distance does the repulsion begin? The following model was employed to study that question. Let $\mathbf{r}(t)$ denote the location of an elk, and $\mathbf{x}(t)$ the location of the ATV, both at time t. Let τ be a time lag to be studied. Consider

$$d\mathbf{r}(t) = \mu(\mathbf{r}(t))dt + \nu(|\mathbf{r}(t) - \mathbf{x}(t - \tau)|)dt + \sigma d\mathbf{B}(t).$$

The times of observation differ for the elk and the ATV. They are every five minutes for the elk when the ATV is present and every one sec for the ATV itself. In the approach, adopted location values, $\mathbf{x}(t)$, of the ATV are estimated for the elk observation times via interpolation. One sees an apparent increase in the speed of the elk, particularly when an elk and the ATV are close to one another.

The processes described so far have been Markov. However, non-Markov processes are sometimes needed in modeling animal movement. A case is provided by the random walk with correlated increments in [28]. One can proceed generally by making the sequence $\{\mathbf{Z}_i\}$ of Equation (26.10) an autocorrelated time series.

A more complex SDE model is described by a functional stochastic differential equation

$$d\mathbf{r}(t) = -\nabla V(\mathbf{r}(t)|H_t)dt + \sigma(\mathbf{r}(t)|H_t)dB(t)$$

with $H_t = \{(t_i, \mathbf{r}(t_i)), t_i \le t\}$ as the history up to time t. A corresponding discrete approximation is provided by

$$\mathbf{r}(t_{i+1}) - \mathbf{r}(t_i) = -\nabla V(\mathbf{r}(t_i)|H_{t_i})(t_{i+1} - t_i) + \sigma\sqrt{t_{i+1} - t_i}\mathbf{Z}_{i+1}$$

with the $\mathbf{Z}_i$ again independent standard Gaussians. With this approximation, a likelihood function may be set down directly and, thereby, inference questions addressed.

It may be that the animals are moving such great distances that the spherical shape of the Earth needs to be taken into account. One model is described in [2]. There may be several interacting particles. In this case, one would make the SDEs of the individual particles interdependent. (References include [13] and [38].)

26.8 Summary

Trajectories exist in space and time. One notices them in many places and their data have become common. In this chapter, two specific approaches have been presented for analyzing such data, both involving SDE motivation. In the first approach, a potential function is assumed to exist with its negative gradient giving the SDE's drift function. The second approach involves setting up a grid and approximating the SDE by a discrete Markov chain moving from pixel to pixel. Advantages of the potential function approach are that the function itself is scalar-valued, that there are many choices for its form, and that knowledge of the physical situation can lead directly to a functional form.

Empirical examples are presented and show that the potential function method can be realized quite directly.

Acknowledgments

References

[1] Anderson-Sprecher, R. (1994). Robust estimates of wildlife location using telemetry data. *Biometrics* 50, 406–416.

[2] Brillinger, D.R. (1997). A particle migrating randomly on a sphere. *J. Theoretical Prob.* 10, 429–443.

[3] Brillinger, D.R. (2003). Simulating constrained animal animal motion using stochastic differential equations. *Probability, Statistics and Their Applications*, Lecture Notes in Statistics 41, 35–48. IMS.

[4] Brillinger, D.R. (2007a). A potential function approach to the flow of play in soccer. *J. Quant. Analysis Sports*, January.

[5] Brillinger, D.R. (2007b). Learning a potential function from a trajectory. *IEEE Signal Processing Letters* 12, 867–870.

[6] Brillinger, D.R., Preisler, H.K., Ager, A.A. Kie, J., and Stewart, B.S. (2001). Modelling movements of free-ranging animals. Univ. Calif. Berkeley Statistics Technical Report 610. Available as www.stat.berkeley.edu

[7] Brillinger, D.R., Preisler, H.K., Ager, A.A. and Wisdom, M.J. (2004). Stochastic differential equations in the analysis of wildlife motion. *2004 Proceedings of the American Statistical Association, Statistics and the Environment Section*, Toronto, Canada.

[8] Brillinger, D.R. and Stewart, B.S. (1998). Elephant seal movements: Modelling migration. *Canadian J. Statistics* 26, 431–443.

[9] Brillinger, D.R., Stewart, B., and Littnan, C., (2006a). Three months journeying of a Hawaiian monk seal. *IMS Collections*, vol. 2, 246–264.

[10] Brillinger, D.R., Stewart, B., and Littnan, C., (2006b). A meandering hylje. Festschrift for Tarmo Pukkila (Eds. E.P. Lipski, J. Isotalo, J. Niemela, S. Puntanen and G.P.H. Styan), 79–92. University of Tampere, Tampere, Finland.

[11] Chandrasekhar, S. (1943). Stochastic problems in physics and astronomy. *Rev. Modern Physics* 15, 1–89.

[12] Durrett, R. (1996). *Stochastic Calculus*. CRC, Boca Raton, FL.

[13] Dyson, F.J. (1963). A Brownian-motion model for the eigenvalues of a random matrix. *J. Math. Phys.* 3, 1191–1198.

[14] Eigethun, K., Fenske, R.A., Yost, M.G., and Paicisko, G.J. (2003). Time-location analysis for exposure assessment studies of children using a novel global positioning system. *Environ. Health Perspec.* 111, 115–122.

[15] Grimmet, G. and Stirzaker, D. (2001). *Probability and Random Processes*. Oxford University, Oxford, U.K.

[16] Guttorp, P. (1995). *Stochastic Modeling of Scientific Data*. Chapman and Hall, London.

[17] Haw, M. (2002). Colloidal suspensions, Brownian motion, molecular reality: a short history. *J. Phys. Condens. Matter* 14, 7769–7779.

[18] Ionides, E.L. (2001). Statistical Models of Cell Motion. PhD thesis, University of California, Berkeley.

[19] Ionides, E.L., Fang, K.S., Isseroff, R.R. and Oster, G.F. (2004). Stochastic models for cell motion and taxis. *Math. Bio.* 48, 23–37.

[20] Jonsen, I.D., Flemming, J.M. and Myers, R.A. (2005). Robust state-space modeling of animal movement data. *Ecology* 86, 2874–2880.

Brillinger et al. 2006b not cited in text.

[21] Kendall, D.G. (1974). Pole-seeking Brownian motion and bird navigation. *J. Roy. Statist. Soc. B* 36, 365–417.

[22] Kurtz, T.G. (1978). Strong approximation theorems for density dependent Markov chains. *Stochastic Process. Applic.* 6, 223–240.

[23] Kushner, H.J. (1974). On the weak convergence of interpolated Markov chains to a diffusion. *Ann. Probab.* 2, 40–50.

[24] Kushner, H.J. (1977). *Probability Methods for Approximations in Stochastic Control and for Elliptic Equations.* Academic Press, New York.

[25] Lai, T.L. and Wei, C.Z. (1982). Least squares estimation in stochastic regression models. *Ann. Statist.* 10, 1917–1930.

[26] Langevin, P. (1908). Sur la théorie du mouvement brownien. *C.R. Acad. Sci.* (Paris) 146, 530–533. For a translation, see Lemons, D.S. and Gythiel, A. (2007). Paul Langevin's 1908 paper. *Am. J. Phys.* 65, 1079–1081.

[27] Lumpkin, R. and Pazos, M. (2007). Measuring surface currents with surface velocity program drifters: the instrument, its data, and some recent results. In *Lagrangian Analysis and Prediction of Coastal and Ocean Dynamics*, eds. Griffa, A., Kirwan, A.D., Mariano, A.J., Ozgokmen, T., and Rossby, H.T., Cambridge University Press, Cambridge, MA.

[28] McCulloch, C.E. and Cain, M.L. (1989). Analyzing discrete movement data as a correlated random walk. *Ecology* 70, 383–388.

[29] Moore, M. (1985). Modelling iceberg motion: a multiple time series approach. *Canadian J. Stat.* 13, 88–94.

[30] Nelson, E. (1967). *Dynamical Theories of Brownian Motion*. Princeton University Press, Princeton, NJ.

[31] Perrin, J. (1913). *Les Atomes*. Felix Alcan, Paris.

[32] Prakasa Rao, B.L.S. (1999). *Statistical Inference for Diffusion Type Processes*. Oxford University, Oxford, U.K.

[33] Preisler, H.K., Ager, A.A., Johnson, B.K. and Kie, J.G. (2004). Modelling animal movements using stochastic differential equations. *Environmetrics* 15, 643–647.

[34] Preisler, H.K., Ager, A.A., and Wisdom, M.J. (2006). Statistical methods for analysing responses of wildlife to distrurbances. *J. Appl. Ecol.* 43, 164–172.

[35] Preisler, H.K., Brillinger, D.R., Ager, A.A. and Kie, J.G. (1999). Analysis of animal movement using telemetry and GIS data. *Proc. ASA Section on Statistics and the Environment*, Alexandria, VA, April 23–25.

[36] Rousseeuw, P.J., Ruts, I. and Tukey, J.W. (1999). The bagplot: a bivariate boxplot. *Am. Statistic.* 53, 382–387.

[37] Sorensen, M. (1997). Estimating functions for discretely observed diffusions: A review. *IMS Lecture Notes Monograph Series* 32, 305–325.

[38] Spohn, H. (1987). Interacting Brownian particles: A study of Dyson's model. In *Hydrodynamic Behavior and Interacting Particle Systems*. (ed. G. Papanicolaou). Springer, New York.

[39] Stark, L.W., Privitera, C.M., Yang, H., Azzariti, M., Ho, Y.F., Blackmon, T., and Chernyak, D. (2001). Representation of human vision in the brain: How does human perception recognize images? *J. Elect. Imaging* 10, 123–151.

[40] Stewart, B., Antonelis, G.A., Yochem, P.K. and Baker, J.D. (2006). Foraging biogeography of Hawaiian monk seals in the northwestern Hawaiian Islands. *Atoll Res. Bull.* 543, 131–145.

[41] Taylor, J.R. (2005). *Classical Mechanics*. University Science, Sausalito, CA.